Relationships between Microvoid Heterogeneity and Physical Properties in Cross-Linked Elastomers: An NMR Imaging Study

Peter Adriaensens, Anne Pollaris, Dirk Vanderzande, and Jan Gelan*

Department SBG, Institute for Materialresearch (IMO), Limburg University, Universitaire Campus, B-3590 Diepenbeek, Belgium

Jeffery L. White

ExxonMobil Chemical, 4500 Bayway Drive, Baytown, Texas 77520-9728

Mauritz Kelchtermans

ExxonMobil Chemical Europe, Hermeslaan 2, B-1831 Machelen, Belgium

Received April 13, 2000; Revised Manuscript Received June 27, 2000

ABSTRACT: ^{1}H NMR imaging experiments identify the presence of microvoids in cross-linked poly(isobutylene−*p*-methylstyrene−*p*-bromomethylstyrene) (PIB-PMS/BrPMS) terpolymers, for both solid and solvent-swollen samples. Three-dimensional reconstruction of the sample images reveals that the voids are spherically shaped. A statistical analysis of the void density in six commercial (i.e., cured and carbon black filled) isobutylene-based elastomers indicates a strong linear correlation between the mechanical performance and the average number of voids per unit area ($R = 0.972$). In addition, the average number of neighboring voids within a radius of 1 mm per void was indicative of mechanical performance ($R = 0.945$). Our experimental results indicate that high microvoid density in cured elastomers leads to crack initiation and accelerated crack growth, thereby resulting in premature mechanical failure of the material. As this relationship is most likely general for many cured polymer compounds, we believe NMR imaging provides a particularly attractive approach to obtaining microvoid densities over bulk length scales in technically important materials.

Introduction

Magnetic resonance imaging (MRI) has become a promising, nondestructive tool for the study of materials.[1] Previous reports on NMR imaging of elastomers have focused on cross-linking and aging in butadiene, styrene−butadiene, or natural rubber and on the analysis of solvent diffusion in elastomer materials.[2−11]

Polyisobutylene-based elastomers such as isobutylene−*p*-methylstyrene−*p*-bromomethylstyrene (PIB-PMS/BrPMS) terpolymers offer promise as a second-generation butyl rubber, since the gas-barrier properties of regular butyl rubber (isobutylene-*co*-isoprene) are maintained, while the resistance to oxidative degradation is enhanced by the saturated polymer backbone.[12] Although the glass-transition temperature T_g of polyisobutylene is comparable to that of polybutadiene or polyisoprene, the chain dynamics are significantly reduced due to the steric constraints associated with interchain packing of methyl groups.[13,14] Due to the short T_2 relaxation time (about 100 μs at ambient temperature) as compared to other elastomers, it is not straightforward to image solid isobutylene-based elastomers using the conventional MRI techniques.[15] As such, MRI data for polyisobutylene and its derivatives are noticeably absent from the literature. One option to circumvent this issue is to reduce the correlation time for chain reorientation by swelling the sample in organic solvents.[6,7,16] Solvent swelling enhances the visualization of morphologically well-defined features, such as voids and cross-link density gradients.

This paper addresses the use of ^{1}H spin echo NMR imaging to study microvoid defects in isobutylene-based elastomers. The ability of multislice NMR imaging to provide data over statistically relevant sample volume (several cm^3) represents a unique advantage over microscopic imaging methods for material property analysis. Morphological data from microscopy methods suffer from an inherently small sampling area, thereby reducing the statistical significance of bulk structure−property relationships. In a previous paper, chemical shift selective images of cured and filled (carbon black) polyisobutylene-based elastomers swollen in a variety of solvents were presented.[11] While it was shown that chemical shift selective imaging of the polymer spins is most sensitive to variations in cross-link density, selective imaging of the swelling solvent proved to be superior for the detection of microvoid defects which appear as dark circular spots in the images. On the basis of a series of different polymer samples, containing both unfilled and filled specimens as well as different curative chemistries, the dark spots appearing in the solvent images could be unambiguously assigned to microvoid defects. Initial data suggested that void density was relevant to the mechanical performance of these elastomer compounds.[11] The goal of this paper is to provide a detailed statistical analysis of the correlation between the mechanical performance and the 3-D NMR imaging void density information (e.g., average number, distribution, and area of voids).

Experimental Section

Materials. The structure of the PIB-PMS/BrPMS terpolymer is shown in Scheme 1. The terpolymer contains 97−98

* To whom correspondence should be addressed.

10.1021/ma000643z CCC: $19.00
Published on Web 08/23/2000

Scheme 1

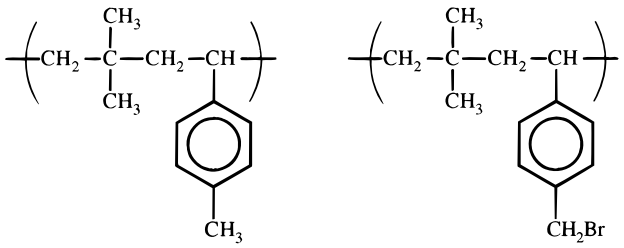

mol % PIB, and as such the chain dynamics and relaxation properties are similar to those of neat polyisobutylene. Cross-linking in this terpolymer occurs through the BrPMS functionality. Inorganic (ZnO) or bifunctional organic curatives (1,6-hexamethylenediamine) may be used to cross-link this terpolymer. The samples used in this study were commercial elastomers, which were cross-linked and filled with carbon black, unless otherwise stated. They have a similar degree of cross-linking as determined by means of the Flory-Rehner method. The mechanical performance criterion used to evaluate these materials was a commercial tire bladder test. In this test, a balloon-type bladder made from the compounds studied here was used to apply pressure against an uncured tire in a tire mold. The bladder compound was pressurized to 200 psi at a temperature of 180−200 °C for a hold time of 11 min. Following this time, the bladder compound was decompressed to ambient pressure for ca. 1 min. Some cooling occurs during this time. In this paper, the number of times this sequence was carried out is denoted as the number of mechanical stress-heat cycles. Failure is defined as the point at which the bladder compound no longer retained pressure, due to air leaks.

NMR Imaging. All MRI images were acquired at 9.4 T on an Inova 400 Varian vertical bore spectrometer equipped with an imaging probe having an inner diameter of 25 mm. Data were obtained at room temperature unless otherwise stated. All two-dimensional images have an in-plane pixel resolution of 100 × 100 μm and a field of view (FOV) of 25 × 25 mm. Images of commercial PIB-PMS/BrPMS samples swollen in C_6H_{12} were obtained with a classical multislice spin-warp pulse sequence (slice selective 90° and 180° sinc pulses) and were used for the 3-D reconstruction and the statistical void density analysis. These slightly T_2-weighted "solvent" images were recorded with a slice thickness of 150 μm, a repetition time TR of 4 s, and an echo time TE of 22 ms. Images of the unfilled 1,6-hexamethylenediamine-cured sample (swollen in C_6H_{12}) were acquired with a slice thickness of 1 mm, TR = 3 s, and TE = 13 ms.

Direct polymer images of the dry, unswollen commercial PIB-PMS/BrPMS terpolymer were obtained using a 16 mm coil with a spin-warp pulse sequence, a slice thickness of 1.5 mm, TE = 2.15 ms, TR = 1 s, and at a temperature of 333 K. Afterward, the same sample was swollen in cyclohexane, and images were recorded as described for the 1,6-hexamethylenediamine-cured sample.

To eliminate local differences in the rubber sample and to obtain reproducible, volume-averaged information, the void density analysis was performed on as many slices as possible. For this purpose, three cylindrical samples of each rubber type with a diameter of 15 mm and height of about 5 mm were examined, representing a total sampling volume of about 2.6 cm^3 for each sample. Such a large sampling volume ensures that the conclusions drawn from the experiments are relevant for the bulk material and represents an important distinction from previous work in this area. Statistical analyses were performed on a Macintosh computer with a flexible imaging analysis program obtained from the National Institute of Health (NIH). For each of the 150 μm slices, the following information was extracted: number of voids, average diameter of the voids, average number of neighbors within a radius of 1 mm per void, and the percent area of the slice taken by voids. These results were finally averaged over all slices to obtain reproducible, volume-averaged information.

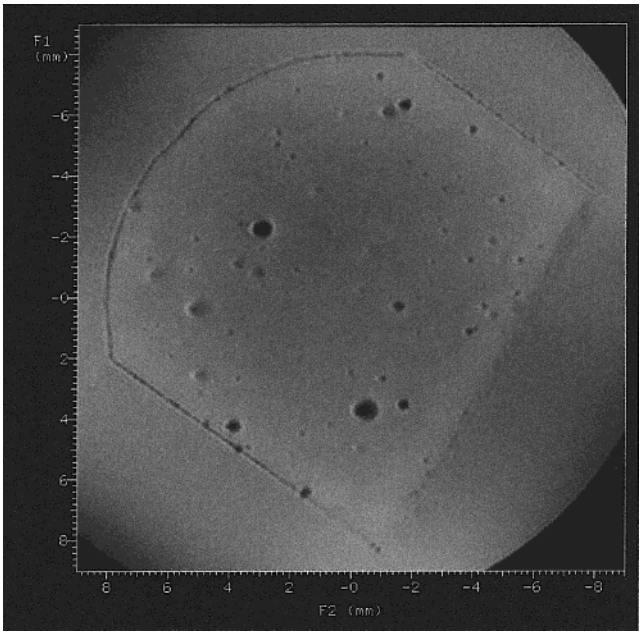

Figure 1. Solvent MRI images of an unfilled, organic (diamine) cured PIB-PMS/BrPMS terpolymer, swollen in cyclohexane.

To perform the 3-D reconstruction, all 150 μm slices were stacked on top of each other to reconstruct a three-dimensional cylinder using the imaging analysis computer program obtained from the National Institute of Health. The program further allows visualizing slices in any direction of the reconstructed cylinder.

Results and Discussion

In a previous paper, chemical shift selective images of a series of polyisobutylene-based elastomers swollen in benzene were presented.[11] While it was shown that chemical shift selective imaging of the polymer spins was most sensitive to cross-link density gradients, selective imaging of the swelling solvent proved to be superior for the detection of microvoid defects. Preliminary experiments indicated that void density critically controls the mechanical performance of these elastomer compounds. It was demonstrated that the dark spots (no ^1H signal) in a solvent image of a swollen sample do not arise from filler particles (inhomogeneous dispersion of carbon black) or from poorly dispersed regions of paramagnetic or ferromagnetic centers of the curative (e.g., ZnO agglomerates or iron particles). The signal-free spots are very regular in shape and size and also appear in unfilled samples cured with an organic curative as shown in Figure 1. Moreover, the amount of curative is too small to account for the area occupied by these spots. For the swollen samples, surface tension prevents the solvent from entering the voids.

Direct proton images of the polymer spins in the absence of any swelling solvent unambiguously confirm that the voids are inherent in these compounded elastomers and do not arise from the swelling process itself (Figure 2a). Figure 2b shows an image of the sample in Figure 2a after swelling in cyclohexane. Although both the solvent and rubber resonances are imaged simultaneously by using cyclohexane as swelling solvent, image intensity is clearly dominated by the solvent. As was already demonstrated, images of a same piece of rubber swollen in C_6H_6 or C_6H_{12} (after drying and

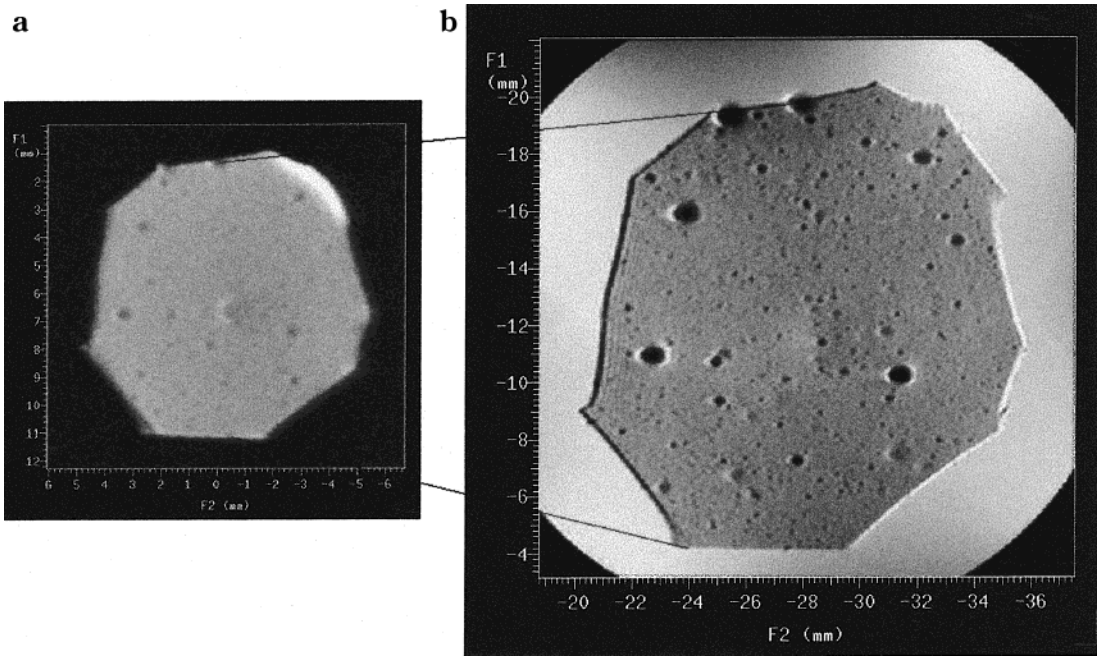

Figure 2. Images of a commercial isobutylene based terpolymer (a) dry, native state and (b) swollen in cyclohexane. The same void locations are clearly observed in both images.

Table 1. Results of a Statistical Void Density Analysis as a Function of the Number of Mechanical Stress-Heat Cycles after Which Failure Occurred for Six Commercial Isobutylene-Based Elastomers[a]

no. of mechanical stress-heat cycles after which failure occurred	av no. of voids detected per cm^2	diameter of the voids (mm)		av no. of neighbors within a radius of 1 mm per void	av area of the slice (%) taken by voids
		average	median		
330	38 ± 14	0.122 ± 0.092	0.100	1.612 ± 1.573	0.798 ± 0.397
318	65 ± 6	0.146 ± 0.137	0.110	2.424 ± 1.753	2.479 ± 0.881
211	80 ± 18	0.143 ± 0.122	0.117	3.112 ± 2.746	2.432 ± 0.883
142	110 ± 8	0.127 ± 0.100	0.098	3.302 ± 1.992	2.274 ± 0.524
89	128 ± 12	0.123 ± 0.094	0.102	4.062 ± 2.371	2.419 ± 0.552
30	135 ± 17	0.131 ± 0.101	0.101	4.072 ± 2.275	2.850 ± 0.520

[a] Values presented are the arithmetic mean and standard deviation, except for the diameter of the voids where also the median is presented. The six elastomers have a similar degree of cross-linking.

reswelling) show the voids in the same positions and with the same dimensions.[11] Figure 2b clearly resolves the black spots at exactly the same positions as in the image of the dry rubber (Figure 2a). Comparing parts a and b of Figure 2 shows that the dimensions of the spots increase by swelling, which again is an indication that the spots are not caused by filler or curative. The larger voids are partially surrounded by bright, crescent-shaped intensity rings that can be ascribed to differences in magnetic susceptibility at the air/polymer interface.[17]

Transverse NMR images of a cyclohexane swollen, commercial terpolymer cylinder are shown in Figure 3. Parts a, b, and c of Figure 3 show a top, central, and bottom 150 μm slice ($x-y$ plane) of the swollen elastomer, respectively. All transverse images were stacked to reconstruct a three-dimensional matrix. Figure 3d shows some longitudinal slices derived from this reconstructed cylinder. The combination of transverse slices (Figure 3a−c) and longitudinal slices (Figure 3d) shows that the voids are indeed spherically shaped. The occurrence of voids in these PIB-PMS/BrPMS terpolymers has also been detected by X-ray microtomography imaging experiments (XRMT) performed on dry polymer samples. A more detailed comparison between MRI imaging and XRMT for the detection of polymer microvoid defects is in progress.

The preceding results demonstrate the presence of several microvoids in the isobutylene matrix, which are inherent to the polymer as a direct result of entrapped air resulting from the low inherent diffusivity of gases in PIB. To look for a correlation between the void density and the mechanical performance of these polymers, a statistical void analysis was performed on six different PIB-PMS/BrPMS terpolymers, having similar cross-link densities. Previous work by Doyle[18] has indicated that the nucleation of small voids is the critical stage for crack growth in natural rubber/EPDM blends. Figure 4a shows a slice from the compound, which underwent 330 stress-heat cycles before failure occurred (failure being defined as the visible formation of multiple cracks). Only a few, rather small voids are observed in the slices of this specimen. The slice shown in Figure 4b on the other hand originates from a specimen which underwent only 30 cycles before failing. The presence of several voids, of which some are excessively large, is observed. Visual inspection of these images already indicates a correlation between the void density and the mechanical performance of the materials.

To obtain reproducible, volume-averaged void density information, a void analysis of 25 slices was performed for three samples of each rubber type, as described above. Several parameters were calculated for each slice: number of voids per cm^2, diameter of the voids,

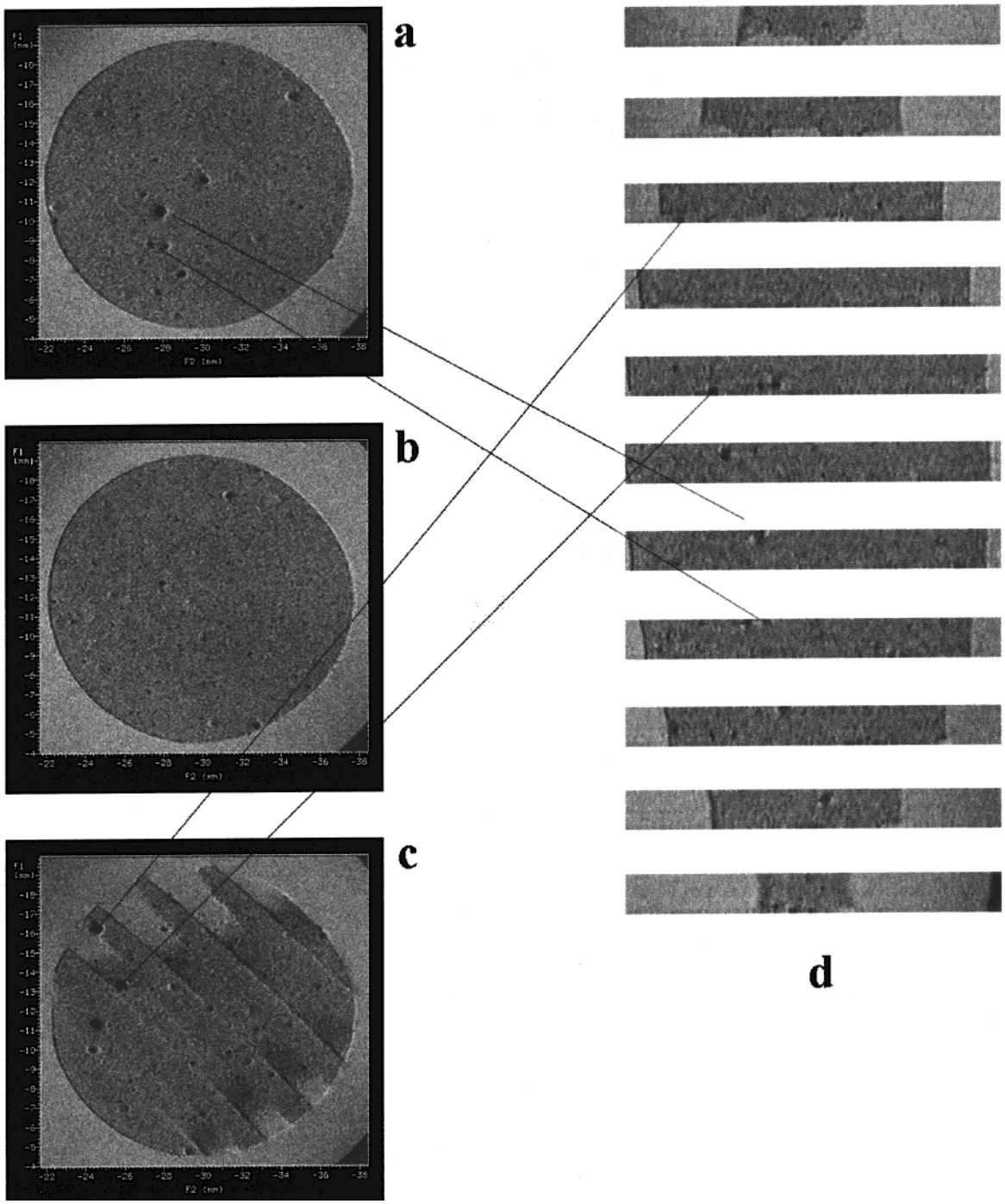

Figure 3. Transverse images of a commercial PIB-PMS/BrPMS terpolymer cylinder, swollen in cyclohexane. Thin slices of 150 μm are shown of (a) a top slice, (b) a central slice, and (c) a bottom slice. All transverse slices were stacked to reconstruct a 3-D matrix from which the longitudinal slices, of which some are presented (d), were derived.

average number of neighbors within a radius of 1 mm per void, and the area of the slice taken by voids. The results obtained upon averaging over all slices are presented in Table 1 for the six terpolymers.

The number of voids detected per cm^2 shows a quasi-normal (Gaussian) distribution with a rather small skewness (<0.3). This is demonstrated in Figure 5, showing the histogram obtained for the terpolymer which underwent 142 cycles. From Figure 6, one can notice a strong linear correlation (correlation coefficient $= 0.972$) between the average number of voids detected per cm^2 and the number of mechanical stress-heat cycles after which specimen failure occurred for the six commercial terpolymers. While the standard deviation is rather similar for all terpolymers, the coefficient of variation (ratio of standard deviation and mean—a measure of the homogeneity of the void distribution over the sample) decreases significantly for samples with a high void density. This means that the voids are distributed rather inhomogeneously in samples with superior mechanical properties (small amount of voids). Although a 2-D analysis of 3-D properties has some limitations, e.g., large voids will be detected in several consecutive slices and will be counted more than once, while small voids having similar x, y coordinates in a slice will be counted only once, a strong correlation is obtained between the number of voids detected per cm^2 and the mechanical performance of the terpolymers.

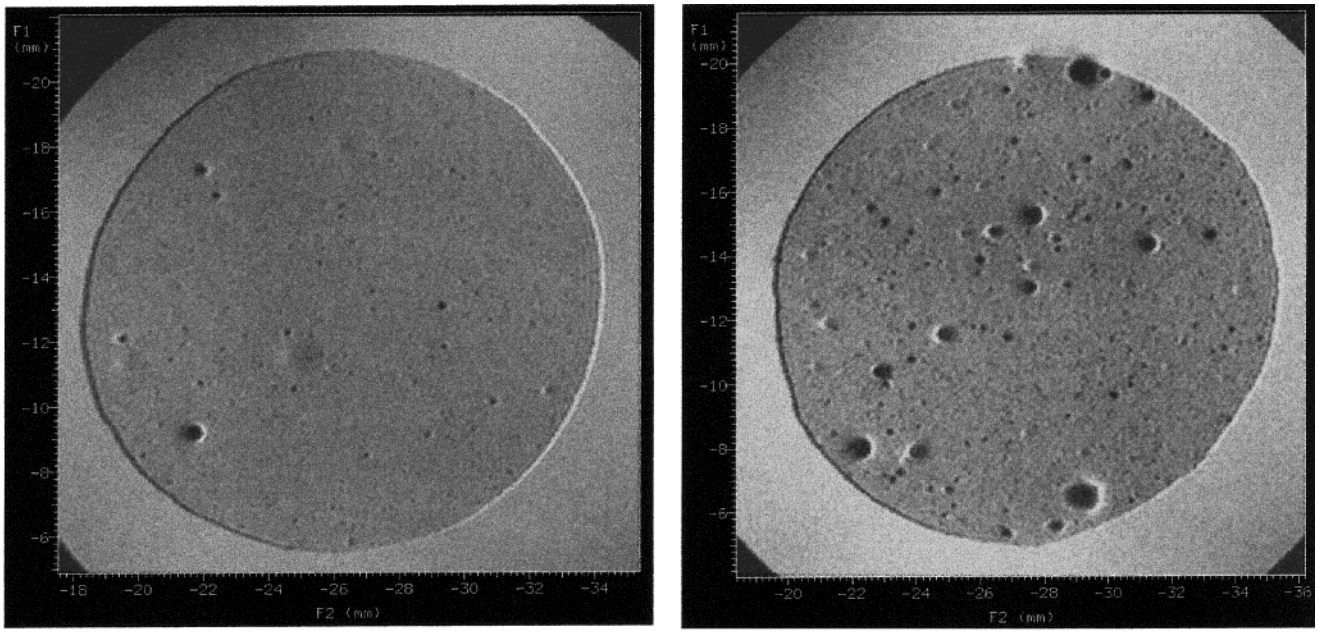

Figure 4. Solvent MRI images of commercial PIB-PMS/BrPMS terpolymers swollen in cyclohexane. The polymers underwent (a) 330 and (b) 30 mechanical stress-heat cycles before failure occurred.

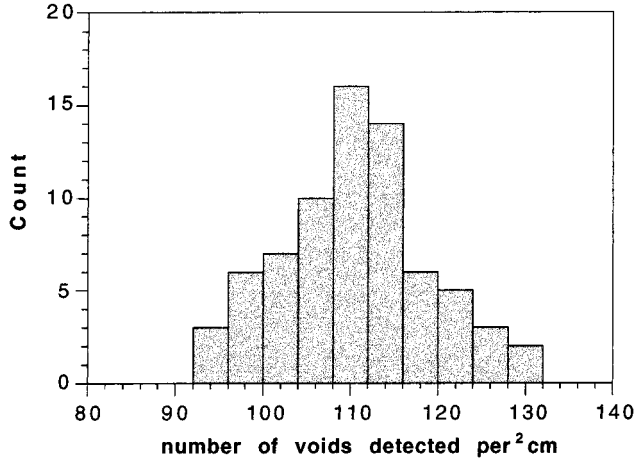

Figure 5. Histogram of the number of voids detected per cm^2 for the terpolymer which underwent 142 stress-heat cycles before failure.

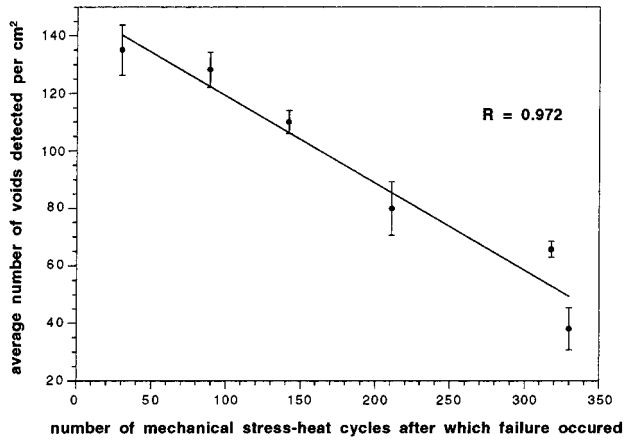

Figure 6. Average number of voids detected per cm^2 as a function of the number of mechanical stress-heat cycle after which failure occurred. The standard deviation is indicated by error bars.

A similar correlation (correlation coefficient of 0.945) is observed between the mechanical performance and the average number of neighbors within a radius of 1 mm per void, a parameter closely related to the average number of voids per unit area. One notes that the distribution of this parameter exhibits skewness, which increases as a function of decreasing average number of neighbors. This is demonstrated in parts a and b of Figure 7, showing the histograms for the terpolymers which underwent 30 stress-heat cycles and 211 stress-heat cycles, respectively. In addition to the inhomogeneous distribution of voids in samples with superior performance (see above), the skewness of the histograms explains the rather high standard deviation reported in Table 1 for this variable. Since stress/strain forces will concentrate near a void, being nucleation sites for craze and crack growth, the presence of a large number of elastomer imperfections will lead to premature failure of the compound since crack propagation probably will be highly oriented toward neighboring voids. MRI experiments as a function of load (elongation) in a home-built stretching device, which allows image acquisition under mechanical stress,[19] are planned to judge the process of crack growth in these unswollen polymer specimens.

Also, the distribution of the diameter of the voids shows a rather high degree of positive skewness, as can be seen in the histograms of Figure 7c,d. Table 1 shows that the average and median diameter of the voids clearly are less critical in terms of mechanical performance. The fourth parameter presented in Table 1 is the average area of the slice (percent) taken by voids, a variable being controlled by the size as well as by the number of voids. Because of severe fluctuations in the void diameter, only a weak correlation with the mechanical performance is observed. Notice the average dimension of the voids in the specimens which underwent 211 and 318 stress-heat cycles (Table 1). These values exceed the "normal" void dimension and results in the deviation from linearity for the average area of

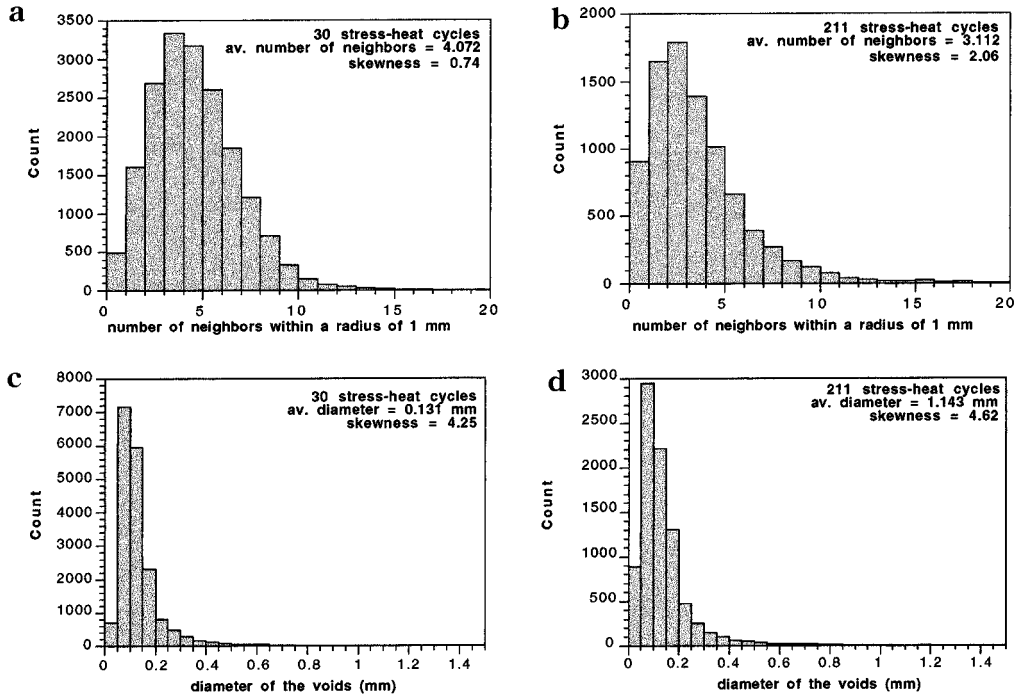

Figure 7. Histograms of the number of neighbors within a radius of 1 mm per void (a, b) and of the diameter of the voids (c, d) for the terpolymers which underwent 30 (a and c) and 211 (b and d) stress-heat cycles before failure.

the slice taken by voids. The data show that the number of voids per cm^2 rather than the diameter of the voids strongly determines the mechanical performance of these commercial elastomer compounds.

Conclusions

Detailed evidence regarding the presence of voids in fully compounded, commercial polyisobutylene-based elastomers is presented. Microvoids are detected in dry and solvent swollen isobutylene-based terpolymers using the ^1H NMR imaging strategy outlined here. The voids have a spherical shape as indicated by a three-dimensional reconstruction of a series of transverse images for each sample. A statistical void density analysis, performed on six commercial isobutylene-based terpolymers, shows that the number of microvoids per unit volume strongly correlates with the mechanical performance of the elastomers ($R = 0.97$). Stress−strain forces will be amplified near a void, thereby creating nucleation sites for craze and crack growth. The presence of a large number of polymer microvoids will lead to undesired physical properties, and NMR imaging has been shown as an effective, nondestructive method for obtaining microvoid density.

Acknowledgment. The authors thank ExxonMobil Chemical for the financial support of this work. This research fits in the framework of the IUAP (Interuniversitaire Attraktiepolen), financed by the Belgium Government (Diensten van de Eerste Minister—Federale diensten voor wetenschappelijke, technische en culturele aangelegenheden).

References and Notes

(1) Blümich, B.; Kuhn, W. *Magnetic Resonance Microscopy*; VCH Verslagsgesellschaft mbH: Weinheim, 1992.
(2) Sarkar, S. N.; Komoroski, R. A. *Macromolecules* **1992**, *25*, 1420.
(3) Blümler, P.; Blümich, B. *Rubber Chem. Technol.* **1997**, *70*, 468.
(4) Fülber, D.; Blümich, B.; Unsfeld, K.; Herrmann, V. *Kautsch. Gummi. Kunstst.* **1995**, *48*, 254.
(5) Kuhn, W.; Barth, P.; Denner, P.; Müller, R. *Solid State Nucl. Magn. Reson.* **1996**, *6*, 295.
(6) Smith, S. R.; Koenig, J. L. *Macromolecules* **1991**, *24*, 3496.
(7) Mori, M.; Koenig, J. L. *J. Appl. Polym. Sci.* **1998**, *70*, 1385.
(8) Rana, M. A.; Koenig, J. L. *Macromolecules* **1994**, *27*, 3727.
(9) Klei, B.; Koenig, J. L. *Acta Polym.* **1997**, *48*, 199.
(10) Ercken, M.; Adriaensens, P.; Vanderzande, D.; Gelan, J. *Macromolecules* **1995**, *28*, 8541.
(11) Adriaensens, P.; Pollaris, A.; Vanderzande, D.; Gelan, J.; White, J. L.; Dias, A. J.; Kelchtermans, M. *Macromolecules* **1999**, *32*, 4692.
(12) Merrill, N. A.; Powers, K. W.; Wang, H. C. *Polym. Prepr.* **1992**, *33*, 962.
(13) White, J. L.; Dias, A. J.; Ashbaugh, J. R. *Macromolecules* **1998**, *31*, 1880.
(14) Boyd, R. H.; Pant, P. V. K. *Macromolecules* **1991**, *24*, 6325.
(15) Ritchey, W. M.; Maylish-Kogovsek, L. *Appl. Spectrosc. Rev.* **1994**, *29*, 233.
(16) Halse, M. R.; Rahman, H. J.; Strange, J. H. *Physica B* **1994**, *203*, 169.
(17) Chang, C.; Komoroski, R. A. *Macromolecules* **1989**, *22*, 600.
(18) Young, D. G.; Doyle, M. J. *Annu. Technol. Conf. Soc. Plast. Eng.* **1992**, *50th Vol. 1*, 1211.
(19) Adriaensens, P.; Storme, L.; Carleer, R.; Litvinov, V. M.; Marissen, R.; Vanderzande, D.; Gelan, J. *Macromolecules* **2000**, *33*, 4836.

MA000643Z